Briefing Space Weather

2023/06/28

1 Sun

1.1 Responsible: José Cecatto

06/12 – No (M/X) flare; Fast wind stream (=< 500 km/s); 6 CME c.h.c. toward the Earth;
06/13 – No (M/X) flare; Fast wind stream (=< 500 km/s); 5 CME c.h.c. toward the Earth *;
06/14 – No (M/X) flare; No fast wind stream; 3 CME c.h.c. toward the Earth;
06/15 – No (M/X) flare; Fast wind stream (=< 700 km/s; 5 CME c.h.c. toward the Earth;
06/16 – M1.0, M1.0, M1.0 flares; Fast wind stream (=< 700 km/); 11 CME c.h.c. toward the Earth;
06/17 – No (M/X) flare; Fast wind stream (=< 600 km/; 7 CME c.h.c. toward the Earth;
06/18 – M1.3, M2.5 flares; Fast wind stream (=< 450 km/s); 7 CME c.h.c. toward the Earth;
06/19 – M1.4, M1.1 flares; Fast wind stream (=< 500 km/s); 5 CME c.h.c. toward the Earth
Prev.: Fast wind stream for the next 01-02 days; for the next 2 days (40% M, 10% X) probability of M / X flares; also,
occasionally other CME can present component toward the Earth.
c.h.c. – can have a component; * partial halo; ** halo
Summary
06/19 – M1.4, M1.1 flares; Fast wind stream (=< 450 km/s); 5 CME c.h.c. toward the Earth;
06/20 – M1.1, X1.1 flares; Fast wind stream (=< 450 km/s); 6 CME c.h.c. toward the Earth *;
06/21 – M1.1, M1.0 flares; Fast wind stream (=< 500 km/s); 13 CME c.h.c. toward the Earth;
06/22 – M1.1, M4.8 flares; Fast wind stream (=< 500 km/s); 4 CME c.h.c. toward the Earth;
06/23 – No (M/X) flare; Fast wind stream (=< 500 km/s); 2 CME c.h.c. toward the Earth;
06/24 – M1.1 flare; Fast wind stream (=< 500 km/s); 5 CME c.h.c. toward the Earth;
06/25 – No (M/X) flare; Fast wind stream (=< 550 km/s); 7 CME c.h.c. toward the Earth;
06/26 – M1.6 flare; Fast wind stream (=< 550 km/s); 6 CME c.h.c. toward the Earth
Prev.: Fast wind stream for the next 01-02 days; for the next 2 days (40% M, 10% X) probability of M / X flares; also,
occasionally other CME can present component toward the Earth.
c.h.c. – can have a component; * partial halo; ** halo

2 Sun

2.1 Responsible: Douglas Silva

- WSA-ENLIL (CME 2023-06-20T17:24 UT)
  - The simulation results indicate that the flank of CME will reach the DSCOVR mission between 2023-06-07T06:14 UT and 2023-06-07T20:14 UT.
- WSA-ENLIL (CME 2023-06-23T00:39 UT)
  - The simulation results indicate that the flank of CME will reach the DSCOVR mission between 2023-06-26T05:00 UT and 2023-06-26T19:00 UT.
- WSA-ENLIL (CME 2023-06-22T13:09 UT)
  - The simulation results indicate that the CME will reach the DSCOVR mission between 2023-06-25T07:16 UT and 2023-06-25T23:16 UT.

Coronal holes (SPOCA):

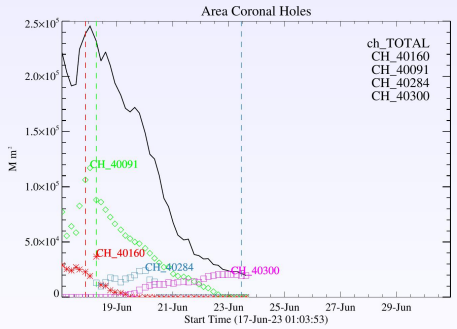

Figura: The solid black line depicts the products of the sum of areas for each detection interval performed by SPOCA between June 17 and 24, 2023.

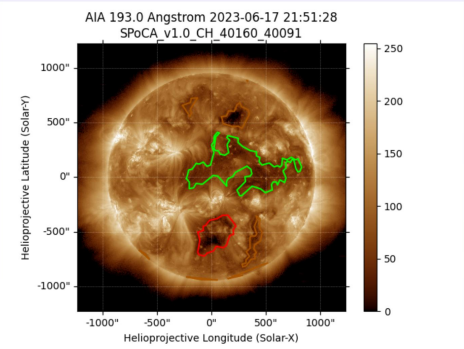

Figura: Above the 193 Å image of the Sun are highlighted coronal holes observed by SPOCA around 21:50 UT on June 17, 2023 (red dot line).

Coronal holes (SPOCA):

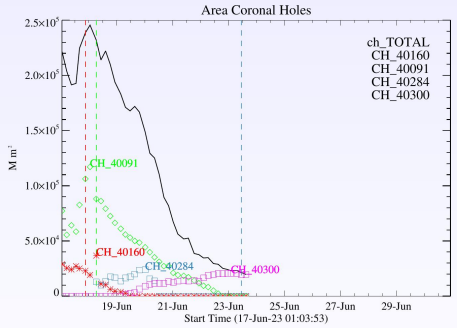

Figura: The solid black line depicts the products of the sum of areas for each detection interval performed by SPOCA between June 17 and 24, 2023.

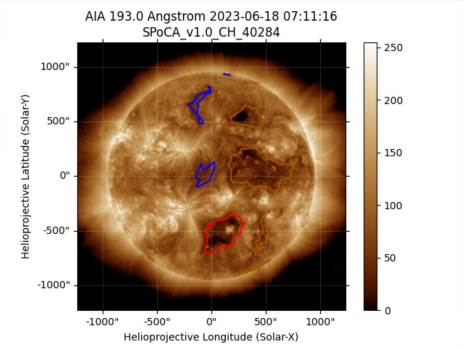

Figura: Above the 193 Å image of the Sun are highlighted coronal holes observed by SPOCA around 07:10 UT on June 18, 2023 (green dot line).

Coronal holes (SPOCA):

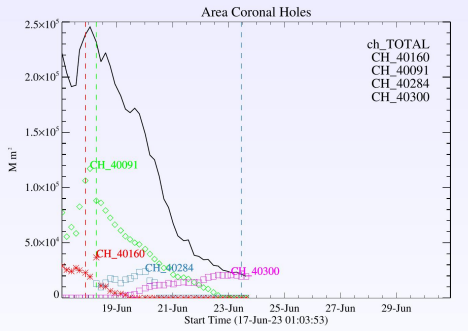

Figura: The solid black line depicts the products of the sum of areas for each detection interval performed by SPOCA between June 17 and 24, 2023.

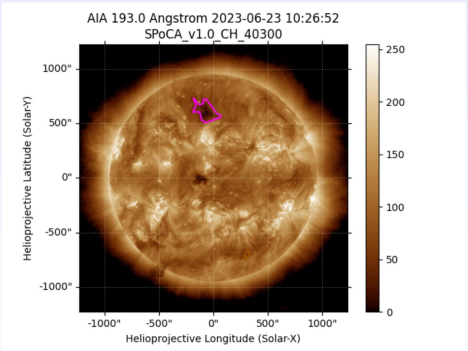

Figura: Above the 193 Å image of the Sun are highlighted coronal holes observed by SPOCA around 10:20 UT on June 23, 2023 (purple dot line).

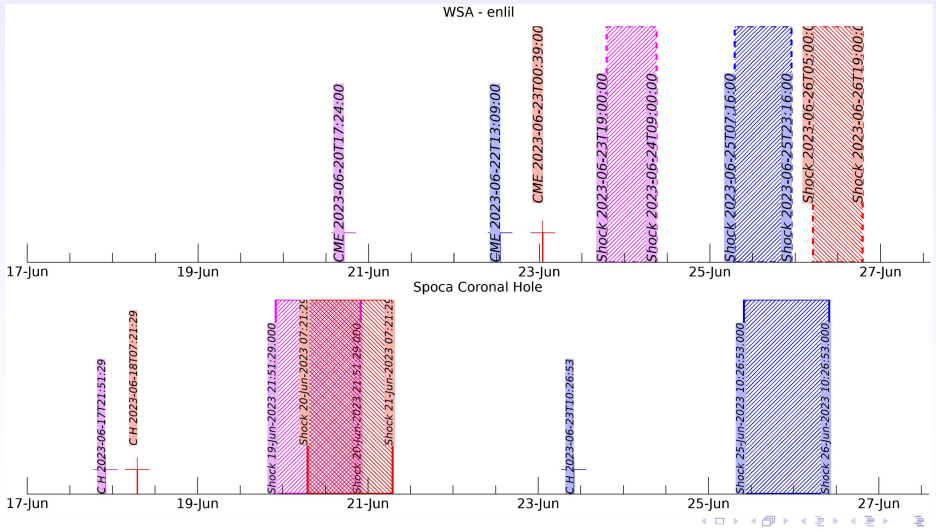

3 Interplanetary medium

3.1 Responsible: Paulo Jauer

- The interplanetary medium region in the last two weeks showed a moderate of plasma perturbations due to the possible interaction of CME and HSS-like structures identified by the DSCOVR satellite in the interplanetary medium.
- The magnitude of the interplanetary magnetic field component on average oscillated below 12 nT. The BxBy components presented variations in the analyzed period, keeping both oscillating within the interval [+10, -10] nT, without the presence of Crossing sector boundary change.
- The bz field component showed variations in the analyzed period and oscillated negatively on average with more evident peaks on June 24 at 04:30 and 22:30 UT.
- The solar wind density fluctuated on average below 12 p/cm^3 with a peak recorded on June 25th at 01:30 of $16p/cm^3$.
- The solar wind speed remained on average above 400 km/s with a peak on June 26 at 20:30 UT of 553 km/s.

- The magnetopause position was oscillating on average above the equilibrium position, with maximum compression on 24/June at 23:30 at 7.9 RE

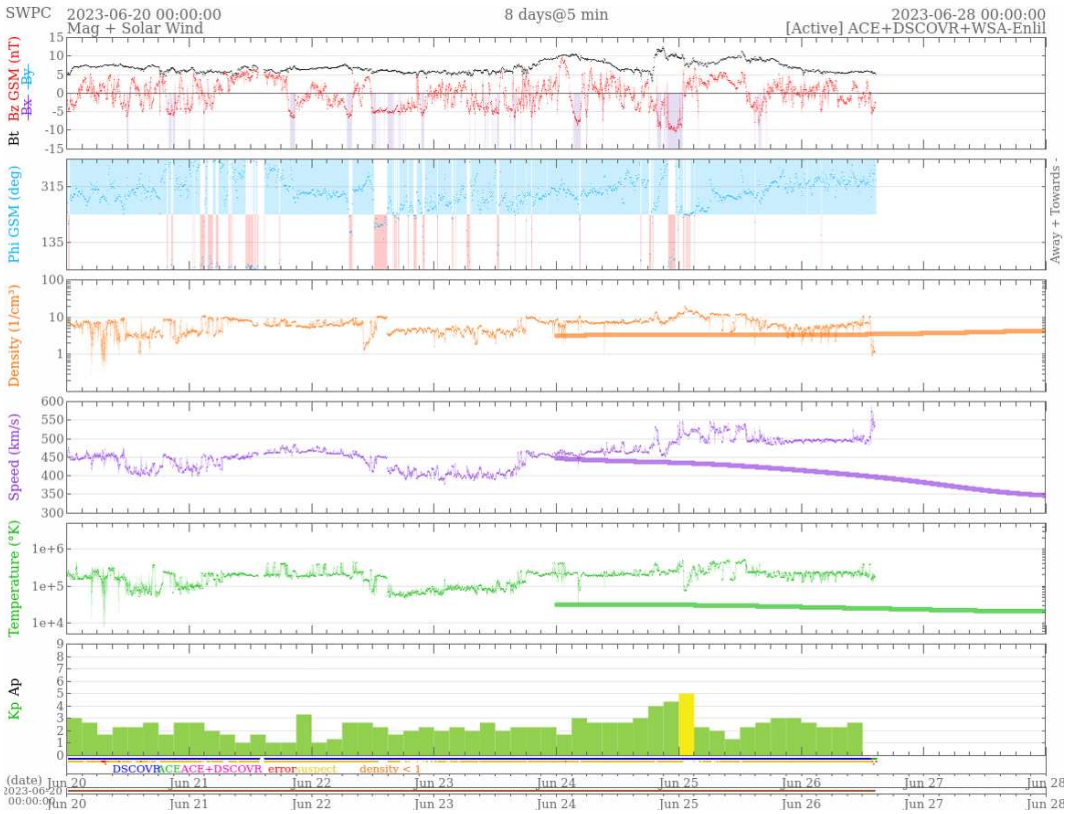

4 Radiation Belts

4.1 Responsible: Ligia Alves da Silva

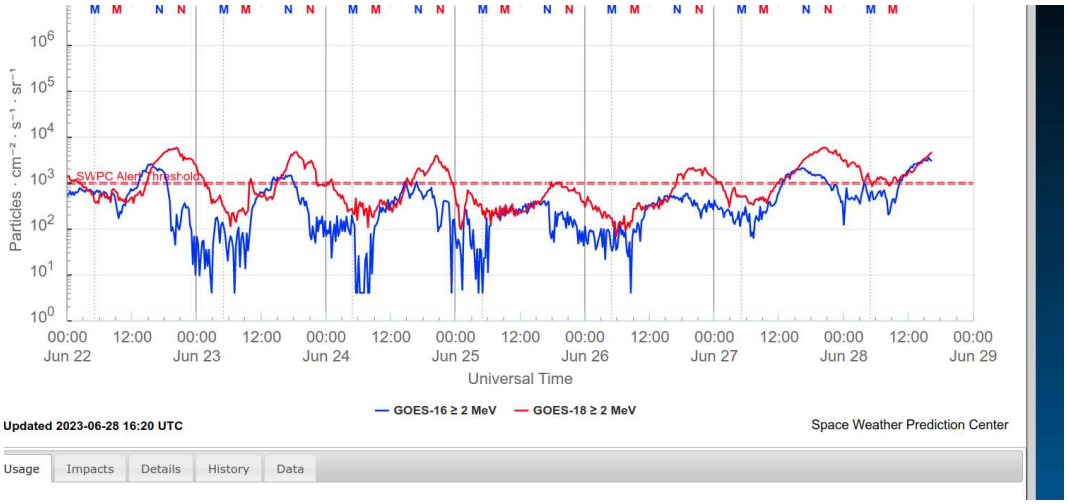

Figura 1: High-energy electron flux (> 2MeV) obtained from GOES-16 and GOES-18 satellite. Source: `https://www.swpc.noaa.gov/products/goes-electron-flux`

High-energy electron flux (> 2 MeV) in the outer boundary of the outer radiation belt obtained from geostationary satellite data GOES-16 and GOES-18 (Figure below) shows two peaks that exceed 10^3 particles/$(cm^2 srs)$ on June 30th and 31st, respectively. A first "dropout" is observed from 00:00 UT on

June 1st, and a second from June 4th. The latter contributes to the confinement of the electron flux to be below 10^2 particles/(cm2 sr) for more than 24 hours.

5 ULF waves

5.1 Responsible: Graziela B. D. Silva

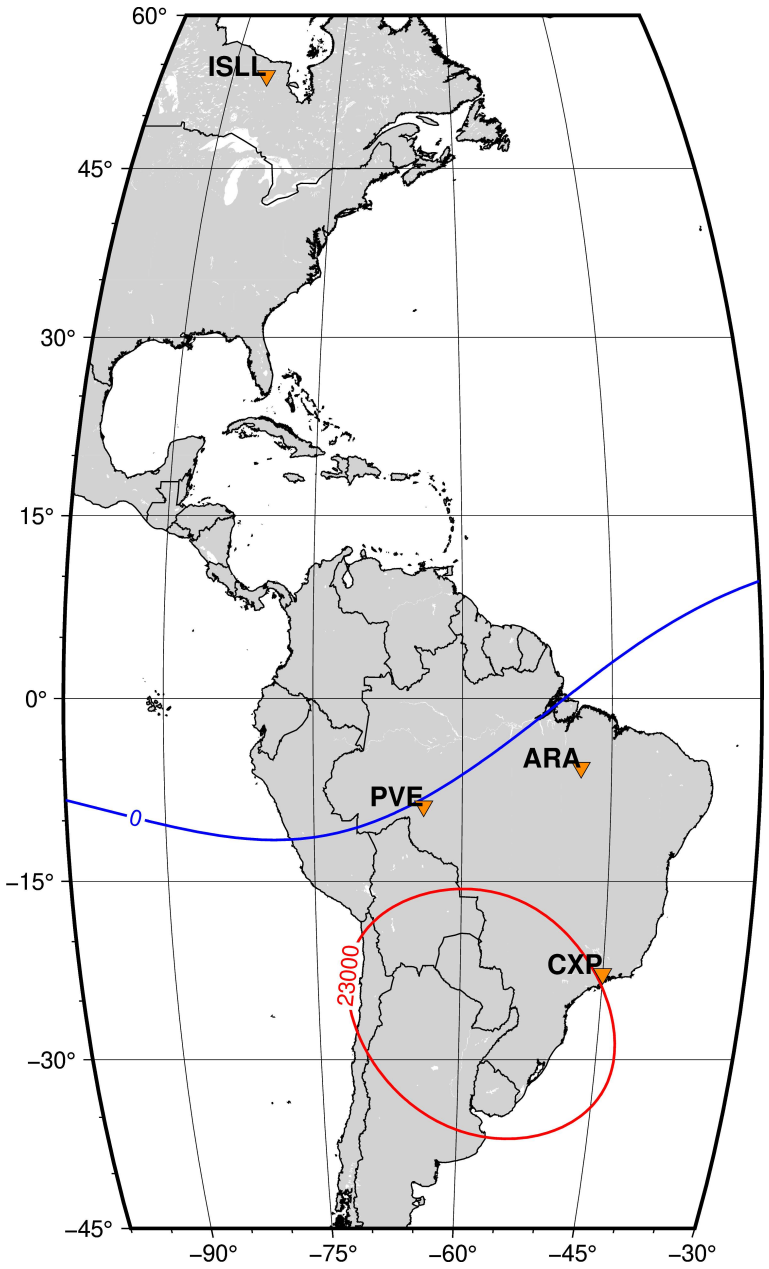

Figura 2: a) Map describing the geographic location of the stations together with the magnetic isolines to show that magnetic equator (blue) and the SAMA region (red). Cortesy: Karen Sarmiento.

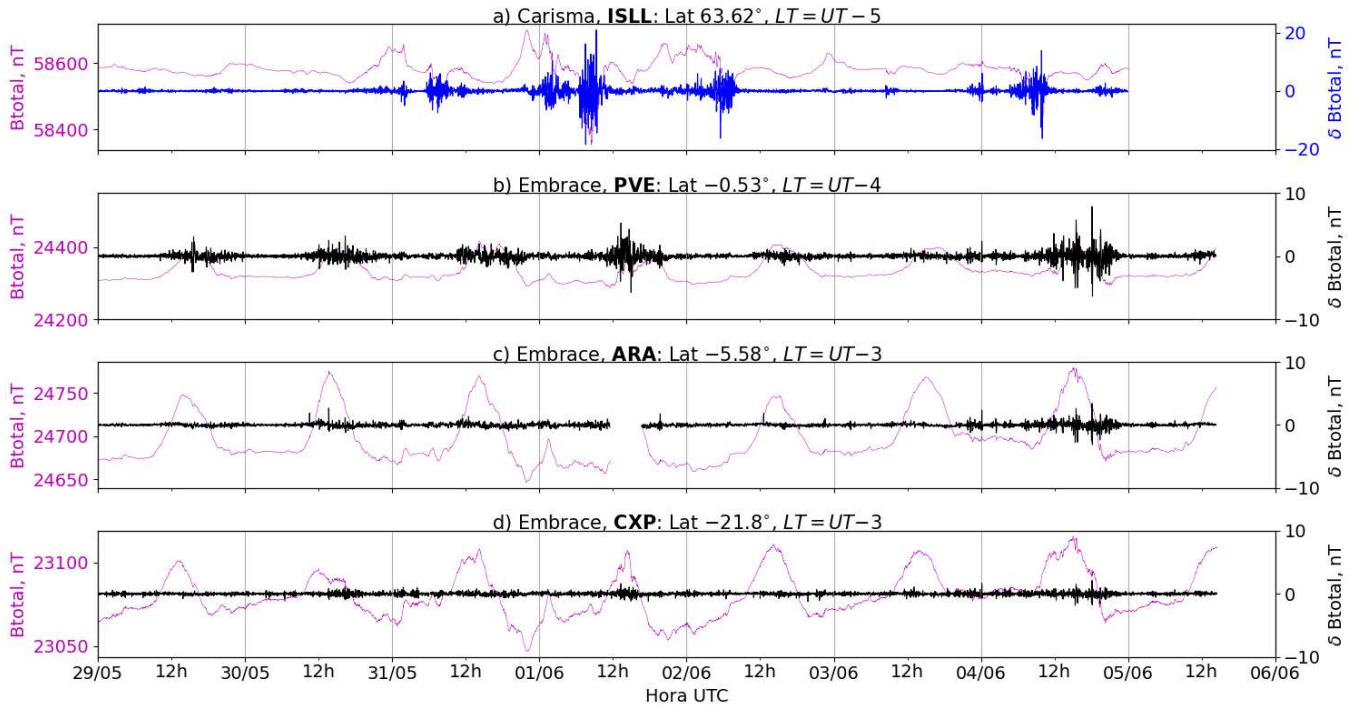

Figura 3: a) Timeseries of the geomagnetic field total component measured at ISLL station (Island Lake) of the CARISMA magnetometer network in magenta, along with the associated perturbation in the Pc5 band shown in blue. b-d) timeseries of the geomagnetic field total component measured at stations PVE (Porto Velho), ARA (Araguatins), and CXP (Cachoeira Paulista) of the EMBRACE network in magenta, along with the Pc5 perturbation in blue.

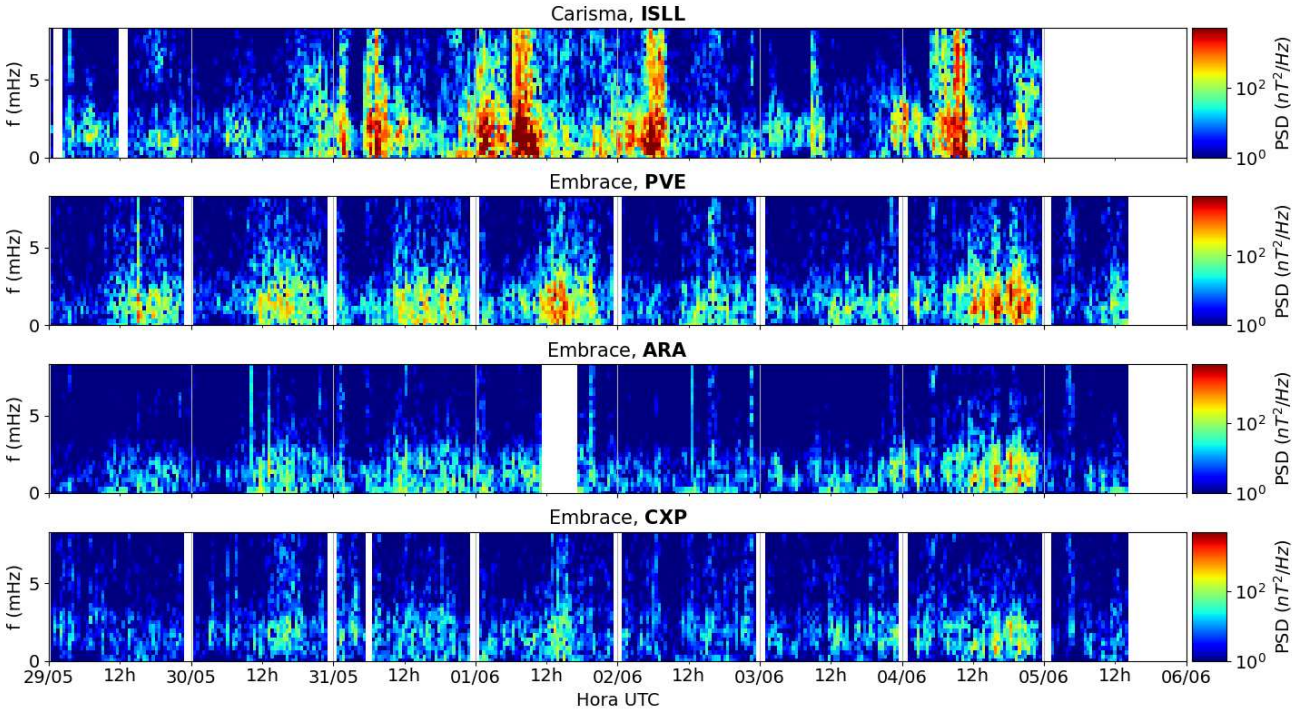

Figura 4: a-d) Time evolution of the power spectral density obtained from the filtered timeseries of the geomagnetic field total component (δ Btotal) for a) the high latitude station (ISLL-CARISMA), and b-d) for the low latitude stations of EMBRACE (PVE, ARA, CXP).

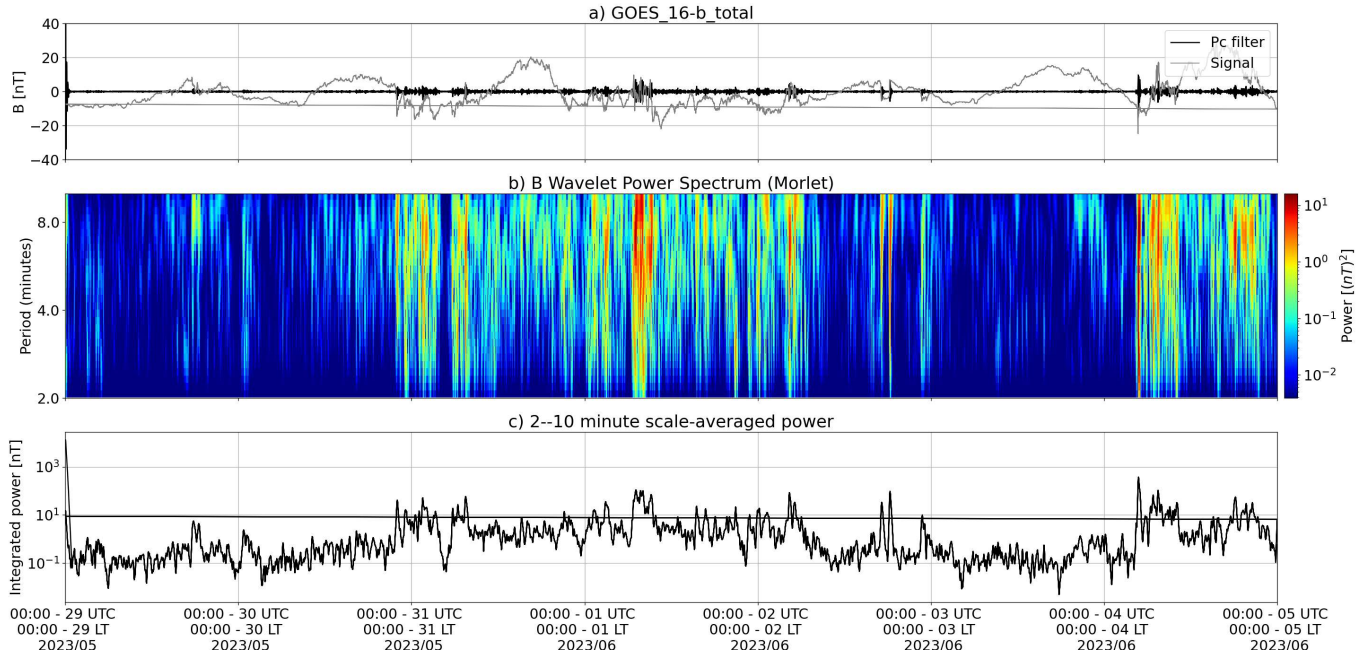

Figura 5: a) Timeseries of the geomagnetic field total component measured by GOES 16, together with the Pc5 fluctuation in black. b) Wavelet power spectrum of the filtered timeseries. c) Average ULF power in the period range from 2 to 10 minutes.

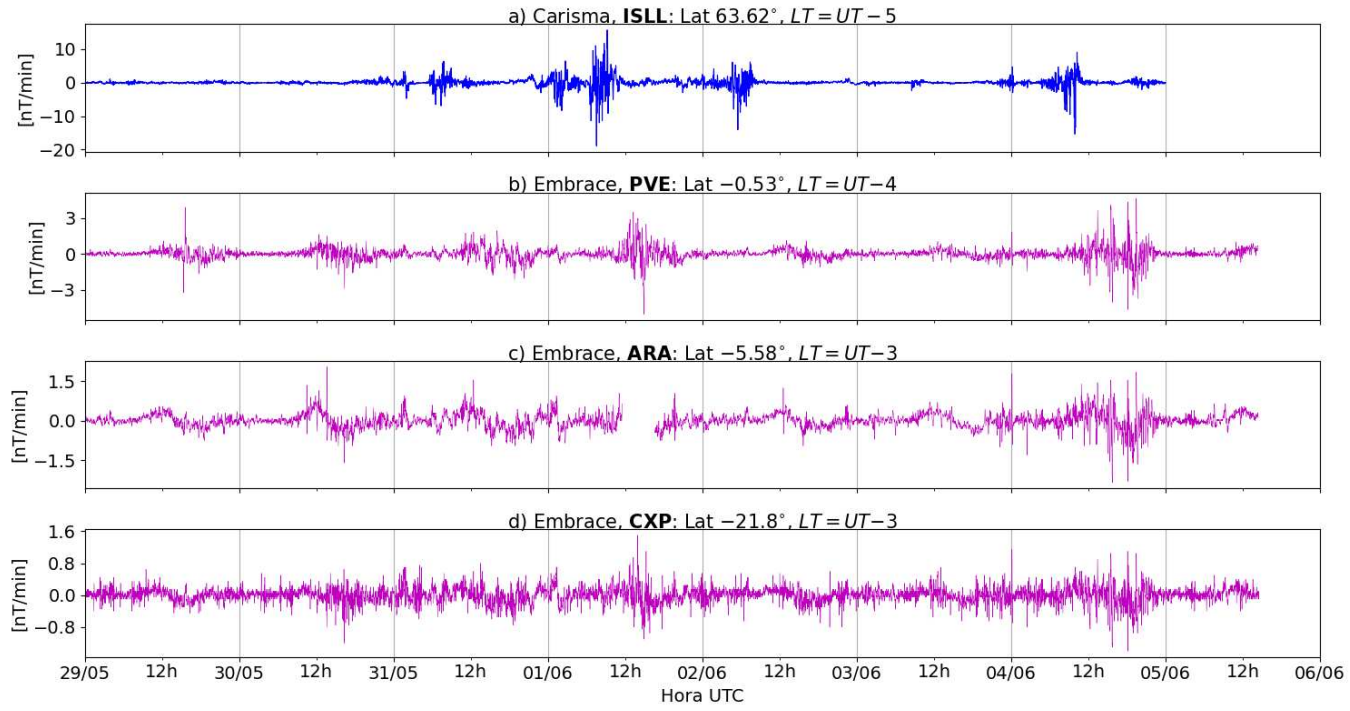

Figura 6: a-d) The rate of change of the geomagnetic field total component (dB/dt) obtained for a) the high latitude station (ISLL-CARISMA), and b-d) for the low latitude stations of EMBRACE (PVE, ARA, CXP).

- The GOES 16 satellite in geosynchronous orbit (L $\sim$ 6.6) registered significant activity of Pc5 ULF waves over the week.
- As observed on the ground, the ISLL station at high latitude registered moderate ULF wave activity

over the week, but acquired low dB/dt activity.

- The PVE station from Embrace MagNet, located under the dip equator, registered significant activity of the waves during the week.
- The CXP and ARA stations at low latitudes of Brazil also registered low activity of the waves over the week, but enhanced activity was reported through June 05 and 11.
- The dB/dt rates were below 6 nT/min in magnitude both at ISLL (high latitude) and the Embrace stations at lower latitudes.
- There was no detection of significant events of SI (sudden impulses or SCs with dB/dt $>$ 5nT/min) over the week.

6 Geomagnetic activity

6.1 Responsible: Lívia Alves

From June 19 to 26, the geomagnetic field was unsettled, the following occurences are highlighted:

- June 23, 24 and 25 Embrace MagNet registered instabilities and a drop of -80 nT in June 25
- jun/24 PVE station registered H-component of -80 nT
- June 24 and 25 AE index reached 1000 nT and Kp was 4o.

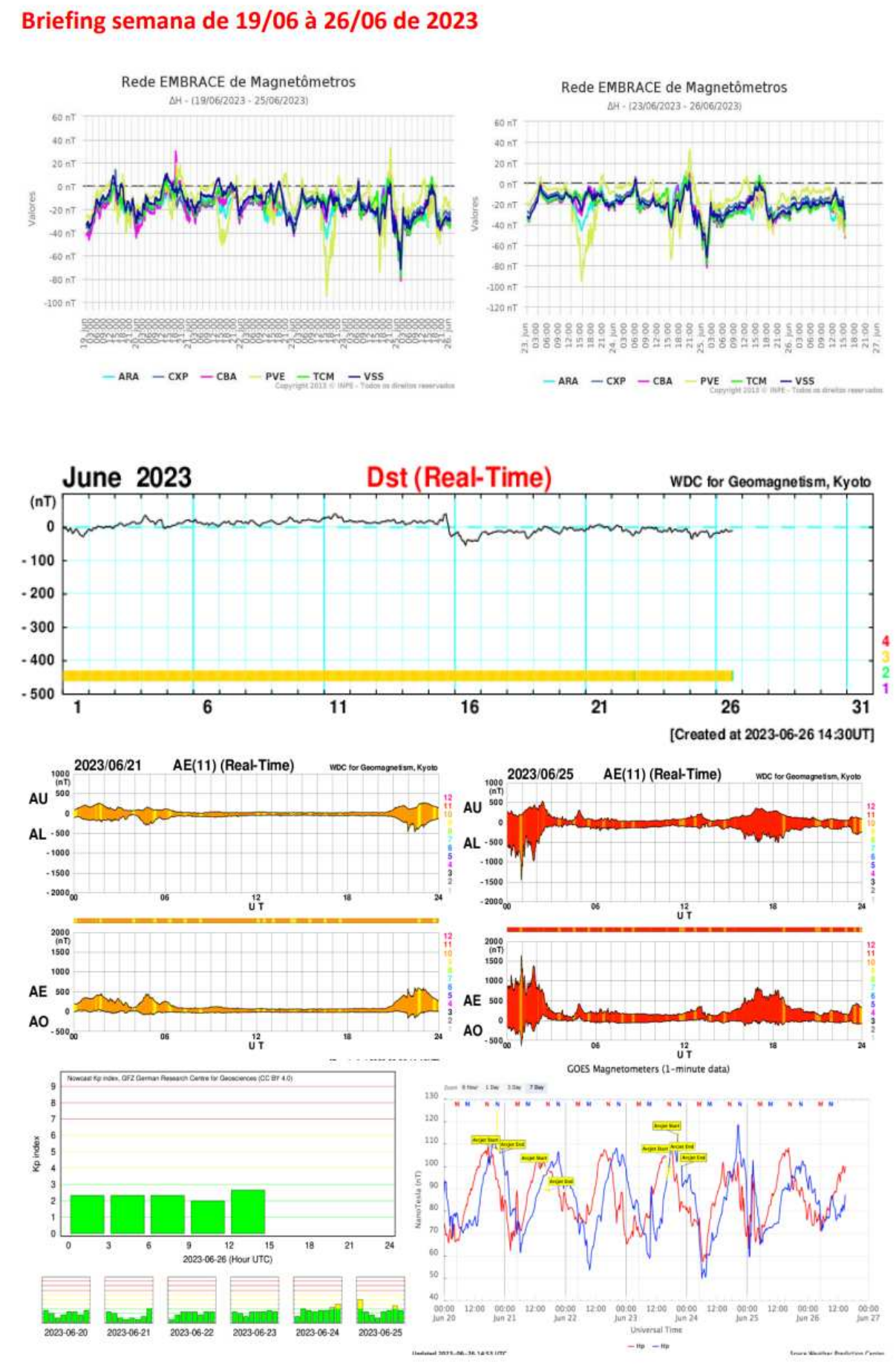

Figura 7: Time evolution of the geomagnetic field data and indices during the reported week.

7 Ionosphere

7.1 Responsible: Laysa Resende

Cachoeira Paulista:

- There were not spread F during this week.
- The Es layers reached scale 4 on days June 22 and 24.

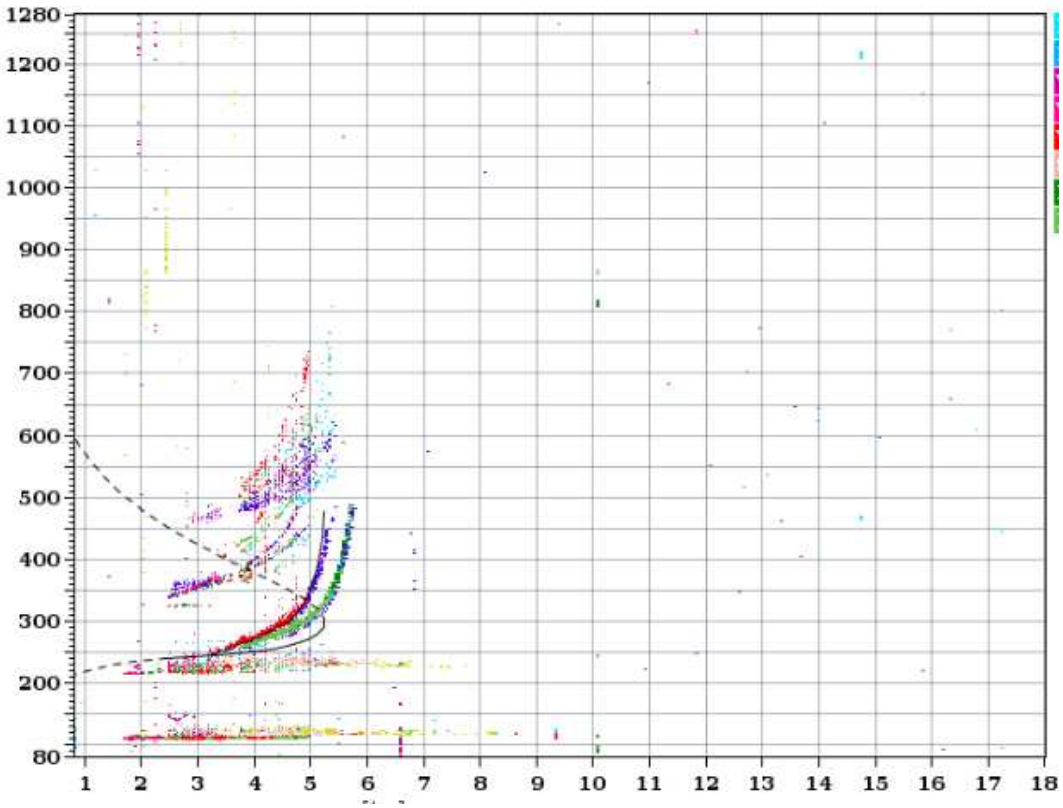

Fortaleza

- There were spread F all days during this week.
- The Es layers reached scale 5 on days on June 21 and 23.

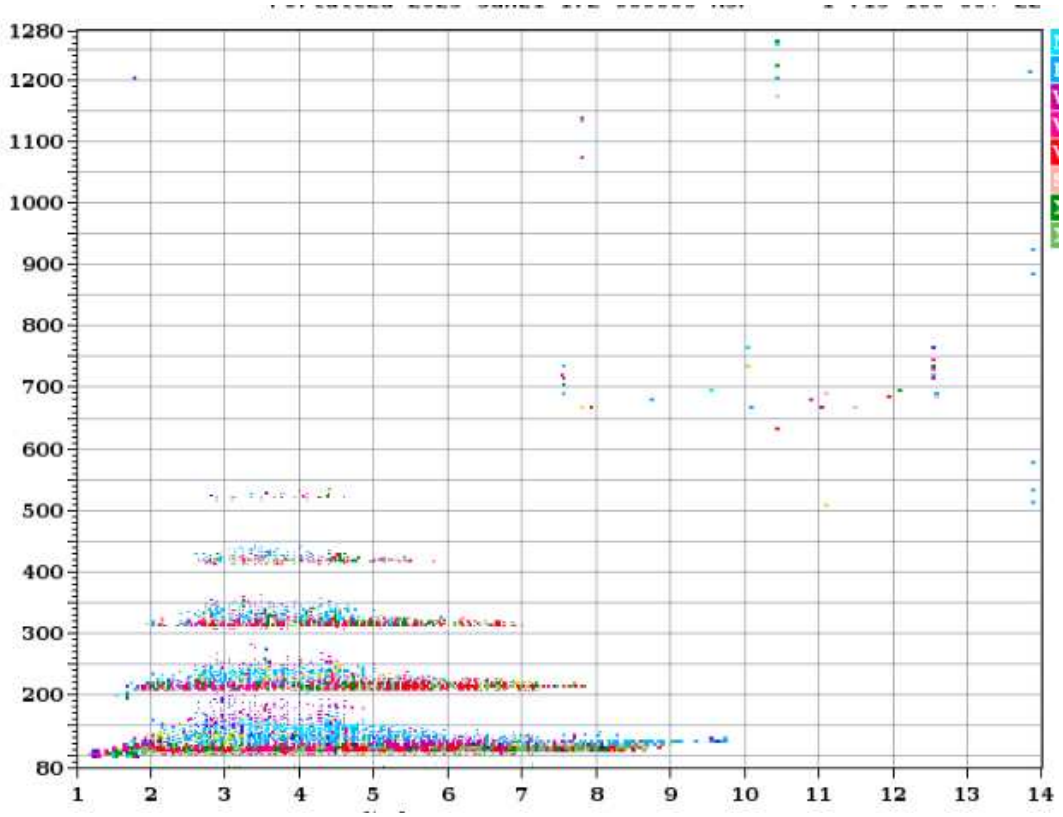

8 Scintilation

8.1 Responsible: Siomel Savio Odriozola

In this report on the S4 scintillation index, data from SLMA in São Luiz/MA, STNT in Natal/RN, STCB in Cuiabá/MT and SJCE in São José dos Campos/SP are presented. The S4 index tracks the presence of irregularities in the ionosphere having a spatial scale $\sim$ 360 m. The S4 index display moderate values only at the STNT station on the 24-25th of this week (Figure 1). In the rest of the stations, the S4 scintillation values remain below 0.3 during the whole week. In the case of the SJCE station, only on the 04/12-13 was recorded strong scintillations. Figure 2 shows the maps with the spatial arrangement of signal interception from some satellites in the GPS constellation, having elevation ¿ 25o, with a layer at 400 km height over the field of view of the STNT stations. This map correspond to the aforementioned date.

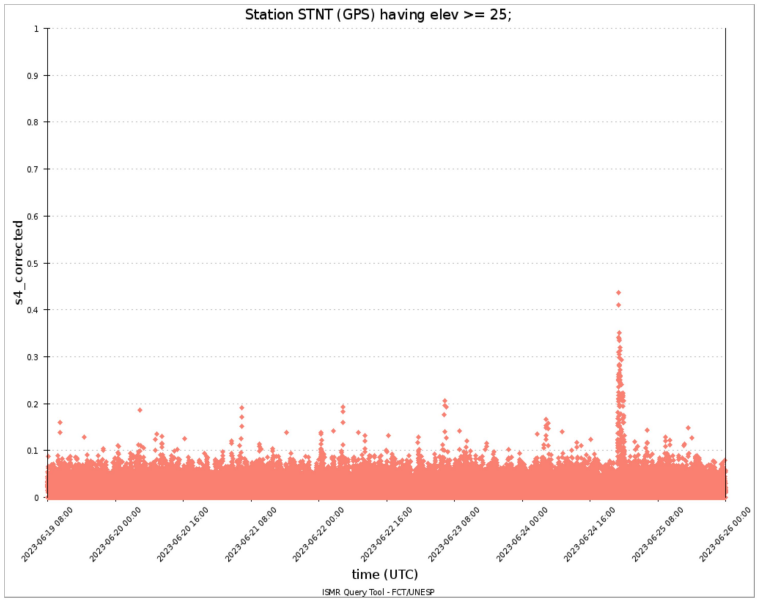

Figure 1: S4 index values for the GPS constellation measured at STNT during the week 06/19--26.

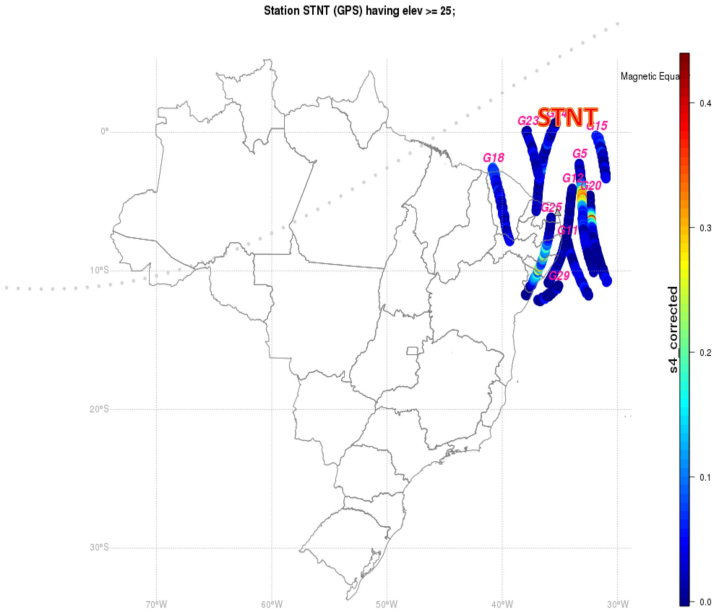

Figure 2: Map of S4 index values for the GPS constellation measured from the point of view of GNSS receiver at STNT from 06/24 at 2200 UT to 06/25 at 0100.

9 ROTI

9.1 Responsible: Carolina de Sousa do Carmo

In the week 2267 (June 18-24, 2023) there were no ionospheric irregularities (plasma bubble), on all analyzed days. Figure below shows the ROTI time series for four stations in the Brazilian sector (Natal (RNNA), Bacabal (MABB), Cuiabá (CUIB) and São José dos Campos (SJSP)).

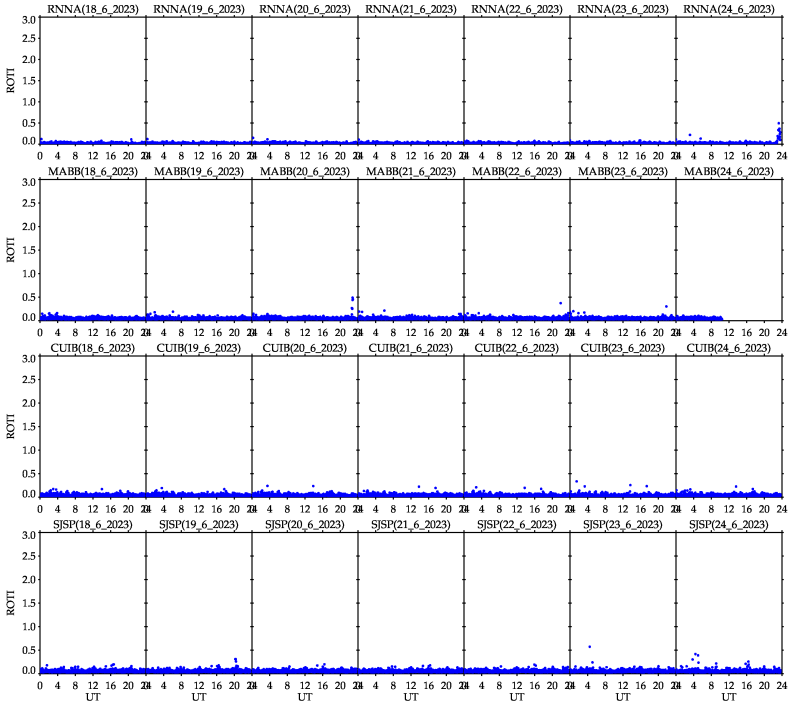

Figura 8: ROTI time series for four stations in the Brazilian sector (Natal (RNNA), Bacabal (MABB), Cuiabá (CUIB) and São José dos Campos (SJSP)), from June 18-24, 2023.